Using data assimilation to understand the effect of disturbance on the carbon dynamics of a managed woodland

Ewan M. Pinnington[1], Eric Casella[3], Sarah L. Dance[1,2], Amos S. Lawless[1,2,4], James I. L. Morison[3], Nancy K. Nichols[1,2,4], Matthew Wilkinson[3], Tristan L. Quaife[1,4]

[1]Department of Meteorology, University of Reading, Reading, UK
[2]Department of Mathematics and Statistics, University of Reading, Reading, UK
[3]Centre for Sustainable Forestry and Climate Change, Forest Research, Alice Holt, Farnham, UK
[4]National Centre for Earth Observation, University of Reading, Reading, UK

Key Points:

- Data assimilation used with the DALEC2 model to investigate effect of selective felling
- New observation operator constructed to allow assimilation of finer temporal resolution information
- No change found in NEE post-disturbance due to concurrent reduction in respiration and GPP

Corresponding author: Ewan M. Pinnington, e.m.pinnington@pgr.reading.ac.uk

Abstract

The response of forests and terrestrial ecosystems to disturbance is an important process in the global carbon cycle in the context of a changing climate. In order to better understand ecosystem response to selective felling (thinning) in a managed forest site we use the mathematical technique of data assimilation to combine a diverse set of observations with a mathematical model of ecosystem carbon balance. We develop new data assimilation techniques allowing for the assimilation of daytime and nighttime net ecosystem exchange observations with a daily time-step model, increasing information available by a factor of 4.25. These techniques allow us to estimate the effect of step-changes in ecosystem composition on the parameter and state variables in a modelled estimate of forest carbon balance. These techniques are applicable to other ecosystem models and data assimilation schemes.

Previous statistical analyses of eddy covariance data at the study site had suggested that disturbance from selective felling resulted in no significant change to the net carbon uptake of the ecosystem. Our results support this with a predicted net ecosystem carbon uptake for the year 2015 of 426 ± 116 g C m^{-2} for the unthinned forest and 420 ± 78 g C m^{-2} for the thinned forest despite a model-predicted reduction in gross primary productivity of 337 g C m^{-2}. We show that this is likely due to reduced ecosystem respiration post-disturbance compensating for a reduction in gross primary productivity. This supports the theory of an upper limit of forest net carbon uptake due to the magnitude of ecosystem respiration scaling with gross primary productivity.

1 Introduction

The response of forests and terrestrial ecosystems to disturbance (e.g. felling, fire, or insect outbreaks) is one of the least understood components in the global carbon cycle [*Ciais et al.*, 2014]. Current land surface models fail to represent the effect of disturbances on long-term carbon dynamics [*Running*, 2008], although these disturbances could have a significant effect on net land surface carbon uptake. Indeed, there could be significant variations in the effect as the range of forest disturbance can be wide: from stand replacing disturbance (where tree mortality is close to 100%) to non-stand replacing disturbance, (where only a proportion of trees are lost). This paper uses data assimilation to improve the modelling of the non-stand replacing disturbance of selective felling (thinning) on forest carbon dynamics.

Thinning is a silvicultural practice used to improve ecosystem services or the quality of a final tree crop and is globally widespread. The effect of thinning on carbon budgets has largely been ignored [*Liu et al.*, 2011]. It would be intuitive to assume that after thinning we would see a reduction in the net carbon uptake of an ecosystem, due to reduced Gross Primary Productivity (GPP) following a reduction in total leaf area and unchanged or heightened ecosystem respiration due to an input of brash and woody debris to the forest floor. However, previous studies, analysing flux-tower eddy covariance records, find no significant change in the observed net ecosystem exchange (NEE) of CO_2 after thinning [*Vesala et al.*, 2005; *Moreaux et al.*, 2011; *Dore et al.*, 2012; *Saunders et al.*, 2012; *Wilkinson et al.*, 2015]. These studies suggest this is due to increased light availability and reduced competition allowing ground vegetation to display increased GPP and compensate for an increase in heterotrophic respiration post-disturbance.

Other studies have shown a significant reduction in the carbon content of rhizosphere soils following tree felling [*Hernesmaa et al.*, 2005]. It has been shown that tree roots provide a rhizosphere priming effect, greatly increasing the rate of soil organic carbon decomposition [*Dijkstra and Cheng*, 2007], suggesting a decrease in respiration following thinning. This is consistent with previous work carried out at the study site in this paper, where it has been shown that the magnitude of ecosystem respiration is strongly coupled to the magnitude of GPP [*Heinemeyer et al.*, 2012]. Predictions made by *Kurz et al.* [2008] about the impacts of mountain pine beetle outbreaks in Northern American forests suggested a switch from sink to source of carbon following this disturbance. However, the analysis of a diverse set of observations for an area with approximately 70% infested trees by *Moore et al.* [2013] revealed little change in net CO_2 flux, due to concurrent reductions in GPP and ecosystem respiration. Similar results were also found from large scale tree girdling experiments [*Högberg et al.*, 2001], where 1-2 months after girdling a 54% decrease in soil respiration was observed.

Here we used data assimilation which is a mathematical technique for combining observations with prior model predictions in order to find the best estimate of a dynamical system. Functional ecology models have been combined with many different observations relevant to the carbon balance of forests [*Quaife et al.*, 2008; *Fox et al.*, 2009; *Zobitz et al.*, 2011; *Richardson et al.*, 2010; *Zobitz et al.*, 2014; *Niu et al.*, 2014; *Pinnington et al.*, 2016], leading to improved estimates of model parameter and state variables and reduced uncertainty in model predictions. Although there have been many efforts to model the ef-

fect of disturbance on forest ecosystems [*Thornton et al.*, 2002; *Seidl et al.*, 2011], the use of data assimilation has been limited to a few examples, all of which used satellite data [*Hilker et al.*, 2009; *Kantzas et al.*, 2015]. The authors are not aware of any studies assimilating site level data to quantify disturbance effects. By assimilating observations relevant to post-disturbance ecosystem carbon dynamics with prior model predictions of ecosystem behaviour, we can analyse the retrieved parameters after data assimilation to find the model predicted effects of disturbance.

In this paper we investigate the effect of thinning on the carbon dynamics of the Alice Holt flux site [*Wilkinson et al.*, 2012], a deciduous managed woodland, following an event in 2014, when one side of the site was thinned and the other side left unmanaged. We present new methods for the assimilation of daytime and nighttime NEE observations with a daily time-step model, in this case the Data Assimilation Linked Ecosystem Carbon (DALEC2) model [*Bloom and Williams*, 2015]. These methods require no model modification. We combine all available observations for 2015 with prior model predictions to find two sets of optimised model parameter and initial state values, corresponding to thinned and unthinned sides of the forest. We then use these two versions of the model to seek to explain why the net uptake of carbon remains unchanged even after removing a large proportion of the trees from one side. We find a net ecosystem carbon uptake for the year 2015 of 426 ± 116 g C m^{-2} for the unthinned forest and 420 ± 78 g C m^{-2} for the thinned forest, despite a reduction in GPP of 337 g C m^{-2} for the thinned forest when compared to the unthinned forest. We find that reduced ecosystem respiration for the thinned forest allows for this unchanged net carbon uptake. The data assimilation techniques presented in this paper could be applied for similar analyses at other sites and provide a novel method to help elucidate the reasons behind ecosystem responses.

2 Observation and data assimilation methods

2.1 Alice Holt research forest

Alice Holt Forest is a research forest area managed by the UK Forestry Commission located in Hampshire, SE England. Forest Research has been operating a CO_2 flux measurement tower in a portion of the forest, the Straits Inclosure, continuously since 1998. The Straits Inclosure is a 90 ha area of deciduous broadleaved plantation woodland located on a surface water gley soil and has been managed for the past 80 years. The ma-

jority of the canopy trees are oak (*Quercus robur* L.), with an understory of hazel (*Corylus avellana* L.) and hawthorn (*Crataegus monogyna* Jacq.), but there is a small area of conifers (*Pinus nigra* ssp. *laricio* (Maire) and *P. sylvestris* L.) within the tower measurement footprint area depending on wind direction. Further details of the Straits Inclosure site and the measurement procedures are given in *Wilkinson et al.* [2012], together with analysis of stand-scale 30 minute average net CO_2 fluxes (NEE) from 1998-2011.

As part of the management regime, the Straits Inclosure is subject to thinning, whereby a proportion of trees are removed from the canopy in order to reduce competition and improve the quality of the final tree crop. At the Straits an intermediate thinning method is used with a portion of both subdominant and dominant trees being removed from the stand [*Kerr and Haufe*, 2011]. The whole of the stand was thinned in 1995. Subsequently the eastern side of the Straits was thinned in 2007 and then the western side in 2014. The flux tower at the site is situated on the boundary between these two sides. This allows for the use of a footprint model to split the flux record and thus analyse the effect of this disturbance on carbon fluxes at the site. In *Wilkinson et al.* [2015] a statistical analysis of the eddy covariance flux record found that there was no significant effect on the net carbon uptake of the eastern side after thinning in 2007. In this paper we focus on the effect of disturbance on the western side after thinning in 2014. We therefore refer to the western side as "thinned" forest and the eastern side as "unthinned" forest.

2.2 Observations

In order to assess the effect the 2014 thinning had on the Straits Inclosure, an intensive field campaign was undertaken in 2015 to measure leaf area index and also to estimate standing woody biomass. From the site we also have a long record of flux data, as discussed in section 2.1. These observations span both the thinned and unthinned sides of the forest.

2.2.1 Leaf area index

To assess the impact of the 2014 thinning, three transects were established in the Straits Inclosure for intensive sampling during 2015. A total of 435 sampling points were marked at 10 m apart, using a GPS and fluorescent tree spray paint. Measurements of peak LAI (July 2015 - September 2015) were made using both a ceptometer and hemi-

spherical photography. The transects were walked twice with the ceptometer taking readings at every sampling point, giving 870 readings in total. Hemispherical photographs were taken every 50 m as shown in Figure 1, giving 89 photographs in total.

We measured below-canopy Photosynthetically Active Radiation (PAR) using the ceptometer while logging above-canopy PAR using a data logger and PAR sensor positioned outside the canopy. We then estimated LAI using the above-canopy and below-canopy PAR readings [*Fassnacht et al.*, 1994]. For the hemispherical photographs, we used the HemiView software [*Rich et al.*, 1999] which calculates the proportion of visible sky as a function of sky direction (gap fraction) which it then uses to calculate LAI [*Jonckheere et al.*, 2004].

Six litter traps were also established at points along the transects (positions shown in Figure 1) allowing for comparison with the other methods. These were sampled throughout the leaf-fall season in 2015. We found the LAI derived from the litter traps was always greater than LAI estimated from optical methods, as expected [*Bréda*, 2003]. From the sampling of the litter traps we also have estimates of leaf mass per area for use in data assimilation. As the 6 litter traps are not enough to describe the LAI for the research site [*Kimmins*, 1973], we used estimates from the ceptometer and hemispherical photographs for data assimilation. We took the weighted average (dependent on number of observations taken of each type) of the hemispherical photograph and ceptometer estimated LAI and derived an LAI of 4.42 with a standard error of 0.07 for the eastern unthinned forest, and an LAI of 3.06 with a standard error of 0.07 for the western thinned forest. We assimilated the mean of 299 LAI observations in the unthinned and 225 in the thinned section of forest. Consequently the appropriate representation of error for data assimilation is the standard error of the mean. From our litter trap observations we find a leaf mass per area of 29 g C m^{-2} free soluble carbohydrates for both sides of the forest.

2.2.2 Woody biomass

The method of Point-Centred Quarters (PCQ) was used to conduct a biomass survey as specified in *Dahdouh-Guebas and Koedam* [2006]. Along the three transects 114 points were sampled measuring the Diameter at Breast Height (DBH) and the density of trees. We then used allometric relationships between DBH and total above ground biomass and coarse root biomass, found in work carried out by Forest Research and in *McKay et al.*

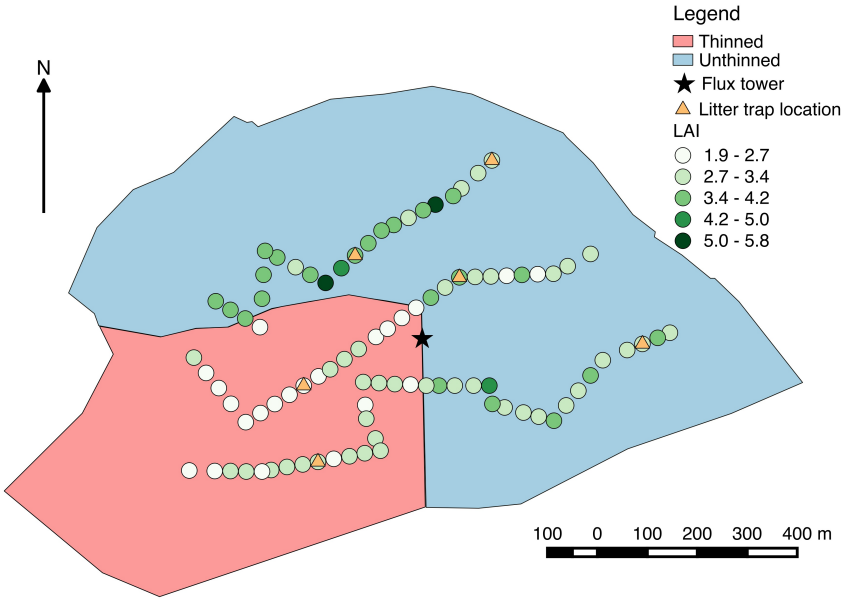

167 **Figure 1.** LAI derived from hemispherical photographs for the Straits Inclosure at 50m intervals along
168 three transects.

175 [2003], to find an estimate of total woody and coarse root carbon (referred to as C_{woo} in
176 the DALEC2 model). These observations are shown in table 1.

177 Forest Research have carried out their own mensuration studies at the site. One such
178 study of the western thinned forest (at a similar time to our own PCQ measurements)
179 found a tree density of 225 ha^{-1} and an average DBH of 32 cm, which are in close agree-
180 ment to the estimates in table 1. This gives us confidence that earlier measurements taken
181 by Forest Research before the thinning are representative of the methods we have used.
182 Measurements of the same section of forest from 2009 found a tree density of 418 ha^{-1}
183 and an average DBH of 28 cm. This suggests that approximately 46% of trees have been
184 removed during the 2014 thinning. From these estimates we can also see the effect thin-
185 ning has on the type of trees found at the site. The trees per hectare has dropped dramat-
186 ically after thinning but the mean DBH has increased, because the smaller subdominant
187 trees have been removed. The greater mean DBH of the eastern unthinned section, 34 cm,
188 indicates that the thinning that took place in 2007 has allowed the dominant trees to grow
189 as a result of reduced competition.

Table 1. Point-centred quarter method observations for 2015.

Sector	Tree density (ha^{-1})	Mean DBH (cm)	Estimated woody biomass and coarse root carbon (g C m^{-2})
Unthinned (E)	272	34.12	13130
Thinned (W)	225	32.85	9908

2.2.3 Flux tower eddy covariance

The Straits Inclosure flux tower provides half-hourly observations from January 1999 to December 2015. These consist of the NEE fluxes and meteorological driving data of temperature, irradiance and atmospheric CO_2 concentration for use in the DALEC2 model. The NEE data was subject to u^* filtering (with a value of 0.2 m s^{-1}) and quality control procedures as described by *Papale et al.* [2006], but was not gap-filled. The resultant half-hourly NEE dataset was then split between observations corresponding to the western thinned and eastern unthinned sides of the site using a flux-footprint model, see *Wilkinson et al.* [2015] for more details.

To match the time-step of our model we computed daily NEE observations by taking the mean over the 48 measurements made each day, selecting only days where there is no missing data. As we have been strict on the quality control of the flux record and not used any gap filling, this presented a problem in terms of the number of daily NEE observations available. By further splitting the flux record between two sides we retrieved very few total daily observations of NEE for either side. In order to address this we computed day and nighttime NEE fluxes (NEE_{day} and NEE_{night} respectively) for use in data assimilation. We used a solar model to define whether NEE measurements were made at daytime or nighttime. We then took the mean over the half-hourly day or nighttime measurements, again only taking periods where there were no gaps in the data so that we were only considering true observations. This provided us with many more observations of NEE for assimilation, as seen in table 2. Because we are averaging over shorter time periods we have a smaller probability of gaps and erroneous data. We see that we have more daytime NEE observations than nighttime, as we tend to have much more turbulent

air mixing in daylight hours. In section 2.3.2 we give details of how we relate these twice daily observations of NEE to a daily time-step model.

Table 2. Number of observations of NEE, NEE_{day} and NEE_{night} for East and West sides of the Straits Inclosure for the year 2015.

Sector	NEE	NEE_{day}	NEE_{night}
Unthinned (E)	22	60	42
Thinned (W)	26	54	48

The errors in observations of daily NEE were assumed to be constant and set at 0.5 g C $m^{-2}day^{-1}$ by *Williams et al.* [2005], whereas *Braswell et al.* [2005] found these errors to be closer to 1 g C $m^{-2}day^{-1}$. However, *Richardson et al.* [2008] show that flux errors are heteroscedastic. To account for the heteroscedastic nature of NEE errors we define an error function that scales between 0.5 to 1 g C $m^{-2}day^{-1}$ based on the magnitude of the observation. This function is defined as $0.5 + 0.04|\text{NEE}^i_{\text{day}}|$ g C $m^{-2}day^{-1}$, where $|\text{NEE}^i_{\text{day}}|$ is the magnitude of the daytime NEE observation. *Raupach et al.* [2005] comment that nighttime measurements of NEE are much more uncertain than daytime measurements. This is difficult to quantify, but here we assume that nighttime flux errors are 3 times the magnitude of daytime errors. We therefore have the error function of $1.5 + 0.12|\text{NEE}^i_{\text{night}}|$ g C $m^{-2}day^{-1}$, where $|\text{NEE}^i_{\text{night}}|$ is the magnitude of the nighttime NEE observation. We also include correlations in time between the errors in our observations of NEE, as discussed in *Pinnington et al.* [2016].

2.3 Model and data assimilation

2.3.1 DALEC2 ecosystem carbon model

The DALEC2 model is a simple process-based model describing the carbon dynamics of a forest ecosystem [*Bloom and Williams*, 2015]. The model is constructed of six carbon pools (labile (C_{lab}), foliage (C_{fol}), fine roots (C_{roo}), woody stems and coarse roots (C_{woo}), fresh leaf and fine root litter (C_{lit}) and soil organic matter and coarse woody debris (C_{som})) linked via fluxes. The aggregated canopy model (ACM) [*Williams et al.*, 1997] is used to calculate daily gross primary production (GPP) of the forest, taking me-

239 teorological driving data and the modelled leaf area index (a function of C_{fol}) as argu-
240 ments. Figure 2 shows a schematic of how the carbon pools are linked in DALEC2; full
241 model equations can be found in the appendix, section A.1.

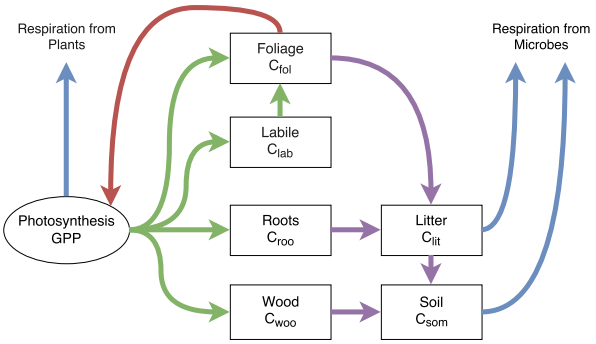

242 **Figure 2.** Representation of the fluxes in the DALEC2 carbon balance model. Green arrows represent C al-
243 location, purple arrows represent litter fall and decomposition fluxes, blue arrows represent respiration fluxes
244 and the red arrow represents the influence of leaf area index in the GPP function.

245 ### *2.3.2 Data assimilation*

246 We implement Four-Dimensional Variational data assimilation (4D-Var) with the
247 DALEC2 model for joint parameter and state estimation [*Navon*, 1998]. In 4D-Var we aim
248 to find the parameter and initial state values such that the model trajectory best fits the
249 data over some time window, given some prior information about the system. This prior
250 information takes the form of an initial estimate of the parameter and state variables of
251 the model, $\mathbf{x}^b$, valid at the initial time. This prior is assumed to have unbiased, Gaussian
252 errors with known covariance matrix $\mathbf{B}$. Adding the prior term ensures that our problem
253 is well posed and that we can find a locally unique solution [*Tremolet*, 2006]. We aim to
254 find the parameter and initial state values that minimise the weighted squared distance to
255 the prior and the weighted squared distance of the model trajectory to the observations,
256 over a time window of length N, with individual time points $t_0,\ldots,t_N$. We do this by
257 finding the state $\mathbf{x}^a$ at time t_0 that minimises the cost function

258 $$J(\mathbf{x}_0) = \frac{1}{2}(\mathbf{x}_0 - \mathbf{x}^b)^T\mathbf{B}^{-1}(\mathbf{x}_0 - \mathbf{x}^b) + \frac{1}{2}\sum_{i=0}^{N}(\mathbf{y}_i - \mathbf{h}_i(\mathbf{x}_i))^T\mathbf{R}_i^{-1}(\mathbf{y}_i - \mathbf{h}_i(\mathbf{x}_i)), \quad (1)$$

where $\mathbf{x}_0$ is the vector of parameter and initial state values to be optimised, $\mathbf{x}_i$ is the vector of model variables at time t_i, $\mathbf{h}_i$ is the observation operator mapping the parameter and state values to the observations, $\mathbf{y}_i$ is the vector of observations at time t_i and $\mathbf{R}_i$ is the observation error covariance matrix. The time step, i, is 1 day in this case. Further details of the implemented data assimilation scheme and specification of prior and observational errors can be found in *Pinnington et al.* [2016].

In this paper we assimilate day and nighttime NEE in order to increase the number of observations available to us and also better partition our modelled estimate of GPP and total ecosystem respiration. As the DALEC2 model runs at a daily time step, this requires us to relate the daily parameter and state values from the model to the twice-daily observations of NEE. We do this by writing two new observation operators, one relating the model state and parameters to daytime NEE, and the other to nighttime NEE. The NEE of CO_2 at any given time is the difference between GPP and ecosystem respiration. For an observation of total daily NEE on day i we have,

$$NEE^i = -GPP^i(C^i_{fol}, \Psi) + f_{auto} GPP^i(C^i_{fol}, \Psi) + \theta_{lit} C^i_{lit} e^{\Theta T^i} + \theta_{som} C^i_{som} e^{\Theta T^i}, \quad (2)$$

where Ψ represents meteorological driving data used the in the calculation of GPP, f_{auto} is the fraction of autotrophic respiration, θ_{lit} is the litter carbon turnover rate, θ_{som} is the soil and organic carbon turnover rate, Θ is the temperature dependence exponent factor and T^i is the mean temperature over 24 hours. Further description can be found in the appendix section A.1. The first term in equation (2) represents gross primary productivity, the second autotrophic respiration and the third and fourth terms heterotrophic respiration.

For total daytime NEE we have,

$$NEE^i_{day} = -GPP^i(C^i_{fol}, \Psi) + \delta_{day} f_{auto} GPP^i(C^i_{fol}, \Psi) + \delta_{day} \theta_{lit} C^i_{lit} e^{\Theta T^i_{day}} + \delta_{day} \theta_{som} C^i_{som} e^{\Theta T^i_{day}} \quad (3)$$

where δ_{day} is $\frac{\text{number of daylight hours}}{24}$, and T^i_{day} is the mean temperature over daylight hours. Here we still have the same term for GPP as in equation (2) as all photosynthesis occurs during daylight hours. We have made the assumption that respiration is spread uniformly in time; therefore the respiration terms are scaled by the fraction of daylight hours. For nighttime NEE we have,

$$NEE^i_{night} = \delta_{night} f_{auto} GPP^i(C^i_{fol}, \Psi) + \delta_{night} \theta_{lit} C^i_{lit} e^{\Theta T^i_{night}} + \delta_{night} \theta_{som} C^i_{som} e^{\Theta T^i_{night}} \quad (4)$$

where δ_{night} is $\frac{\text{number of night hours}}{24}$, and T^i_{night} is the mean nighttime temperature. In equation (2) we do not have a term for GPP as no GPP will occur during the night. The respiration is here is scaled by the fraction of nighttime hours. The length of day and night are calculated using a solar model.

These new observation operators allow for assimilation of day/nighttime NEE without the need for altering the model and can be applied to other ecosystem models to allow for the assimilation of eddy covariance data at a finer temporal resolution.

2.4 Experimental setup

In order to assess the information content of the three available data streams (described in section 2.2) and their impact on the effect of disturbance as predicted by the model, we conducted a data denial procedure. This involved assimilating different combinations of observations, in three experiments, as shown in table 3. In our first experiment we used only the eddy covariance data, as this is the data type most commonly used in data assimilation studies. In the second we added the observations relating to leaf mass and area and finally in the third experiment we added the observations of woody biomass, as NEE observations have been shown to be unable to constrain this [*Fox et al.*, 2009]. In each experiment we used the prior model as specified in the appendix in table A.1. This prior model was found by assimilating daytime and nighttime NEE, leaf mass per area and LAI observations from 2012 and 2013 before the thinning occurred. More information on the methods used to find this prior model can be found in *Pinnington et al.* [2016].

In each experiment we ran the assimilation for both the thinned forest and the unthinned forest, using the distinct data for each side. This allowed us to retrieve a unique set of parameter and initial state values for each section of forest. We analysed the optimised parameter and initial state values for the thinned and unthinned forest and also the model predictions of different variables for each side post-disturbance. This allowed us to judge the effect the thinning in 2014 had on the carbon dynamics of the forest in 2015.

It would be expected that we will retrieve different estimates for each of the experiments outlined in table 3, with our most confident estimate being when all observations types are assimilated together in experiment C. This would allow us to see how much information each data stream provides and assess whether NEE data alone is enough to understand the effect of disturbance.

Table 3. Combination of observations used in data assimilation experiments.

Experiment	NEE	LAI & leaf mass per area	C_{woo}
A	×		
B	×	×	
C	×	×	×

3 Results

In Figure 3 and 4 we show the observations and model trajectories after assimilation for the thinned and unthinned forest for experiments A and C respectively. We can see that the model fits all the assimilated observations well after assimilation for both experiments. We have confidence in our results as we have demonstrated previously that assimilating a single year of data can accurately forecast the carbon uptake of the site for a long time period (15 years) [*Pinnington et al.*, 2016]. From Figure 3a and 3b we see that the modified observation operators presented in section 2.3.2 have allowed our model to represent both daytime and nighttime NEE well.

In experiment A we have only assimilated NEE observations. From table 4 we can see that we improve the fit to the assimilated observations for both the unthinned and thinned forest when compared to the prior model. The root-mean-square error (RMSE) is within the specified observation error for both daytime and nighttime NEE after assimilation. By only assimilating observations of NEE we have not been able to accurately predict LAI. Although we have improved the fit of the model to LAI after assimilation for the thinned forest (see table 4), we have significantly degraded the fit of the model to LAI for the unthinned forest. Partitioning the NEE dataset between the thinned and unthinned forest (as described in section 2.2.3) has resulted in a gap in the observations for the unthinned forest during the period of greatest carbon uptake (June 2015 - August 2015), see Figure 3a. This is due to the prevailing wind in this period being from the south-west. The gap in the NEE dataset when observations would have been of highest magnitude causes our model to under-predict the carbon uptake for the unthinned forest. This bias introduced into the NEE dataset for the unthinned forest results in a significantl under-prediction of LAI, as seen in Figure 3c. From Figure 3d and table 4 we can see that NEE

observations alone do not give us enough information to recover a value of C_{woo} with the DALEC2 model. This is also found in previous work [*Fox et al.*, 2009].

In experiment B we have assimilated observations of NEE, LAI and leaf mass per area. From table 4 we see that including the extra observations have allowed the model to fit LAI well for both the unthinned and thinned forest, and although the fit of the model to the NEE observations is slightly degraded, it is still well within the specified observation error from section 2.2.3. We also see that including these extra observations still does not allow us to recover an accurate value of C_{woo}.

In experiment C we assimilate all available observations. This gives us very similar results as in experiment B, except that including the observations of C_{woo} in the assimilation allows the model to fit this observation well, as seen in table 4. We see from Figure 4a and 4c that including observations of LAI in the assimilation removes the bias introduced from the partitioning of the NEE observations between the unthinned and thinned forest. The distinct difference in stand structure is now clear in Figure 4, with reduced LAI and woody carbon for the thinned forest. For experiment C the time of senescence in LAI predicted by the model is consistent with phenocam observations made by Forest Research at the site, as shown in the supplementary material (Figure S12). However, the time of green-up in LAI predicted by the model is later than the phenocam observations. We hypothesise that this is due to the model predicting the photosynthetically effective LAI implicitly rather than the LAI related to canopy green index measured by the phenocam, which will show present LAI before new leaves become competent at photosynthesis [*Reich et al.*, 1991; *Morecroft et al.*, 2003].

Table 5 shows the cumulative annual fluxes for the year 2015 for the three experiments. In all three experiments there is no significant difference between the net carbon uptake for the thinned and unthinned forest. We can see that both experiments B and C predict very similar cumulative fluxes, suggesting that the assimilated observations of C_{woo} have not had much impact on the model carbon dynamics for this time period. Because the rate parameters controlling this pool are relatively slow it is likely that observations of C_{woo} will become much more important over longer time-scales. Here we have only assimilated a single observation of C_{woo} for either side of the forest; if multiple observations of C_{woo} were available throughout time this would give us an estimate of the rate of woody biomass accumulation, providing an important constraint on the carbon as-

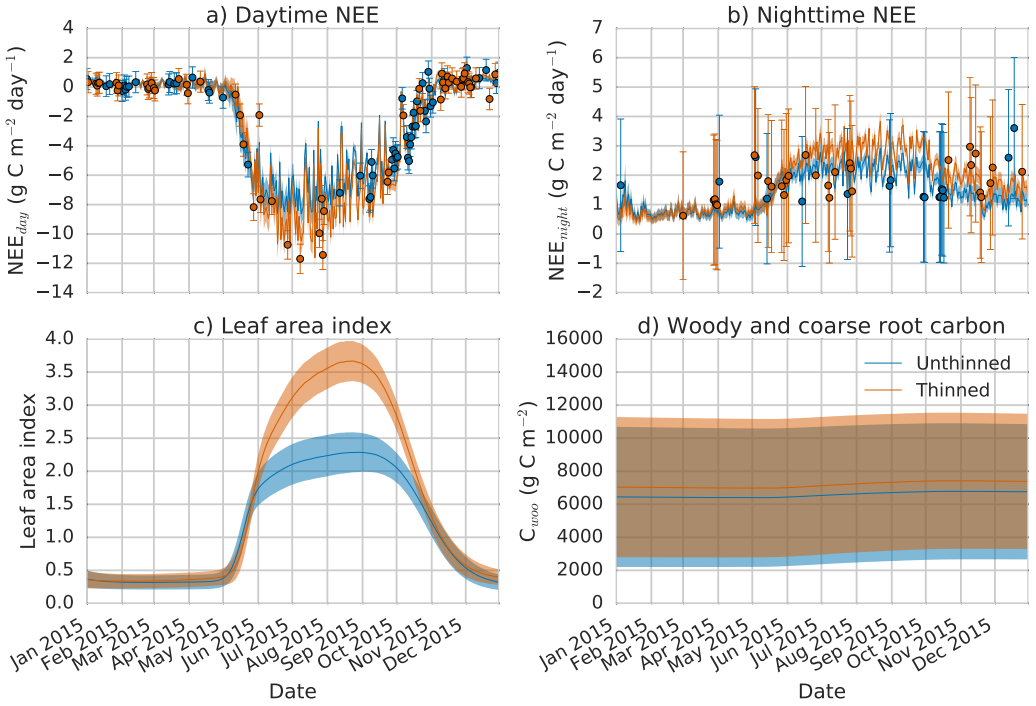

366 **Figure 3.** Experiment A: 2015 unthinned and thinned forest observations and model trajectories after
367 assimilation. Blue line: model trajectory after assimilation of unthinned data, blue shading: uncertainty in
368 model trajectory after assimilation (± 1 standard deviation), blue dots: unthinned observations with error
369 bars, orange line: model trajectory after assimilation of thinned data, orange shading: uncertainty in model
370 trajectory after assimilation (± 1 standard deviation), orange dots: thinned observations with error bars.

386 similation of the forest. Experiments A and C both predict no significant difference in the
387 net ecosystem carbon uptake between the thinned and unthinned forest. However, the par-
388 titioning of this carbon uptake between GPP and total ecosystem respiration (TER) is sig-
389 nificantly different, with experiment A predicting increased TER and GPP after thinning
390 and experiment C predicting reduced TER and GPP after thinning. This can be seen more
391 clearly in Figure 5. The difference between the results of experiment A and C highlights
392 the issue that NEE is the difference between two large fluxes (NEE = -GPP + TER) and
393 we can therefore find an accurate prediction of NEE despite under/overestimating both
394 GPP and TER. Therefore, care should be taken when interpreting model results based
395 solely on NEE data, especially in this case, as we have seen that the partitioning of the
396 NEE data between the thinned and unthinned forest has introduced a bias into our dataset.
397 If we were to base our analysis on experiment A we would assume that the thinning had

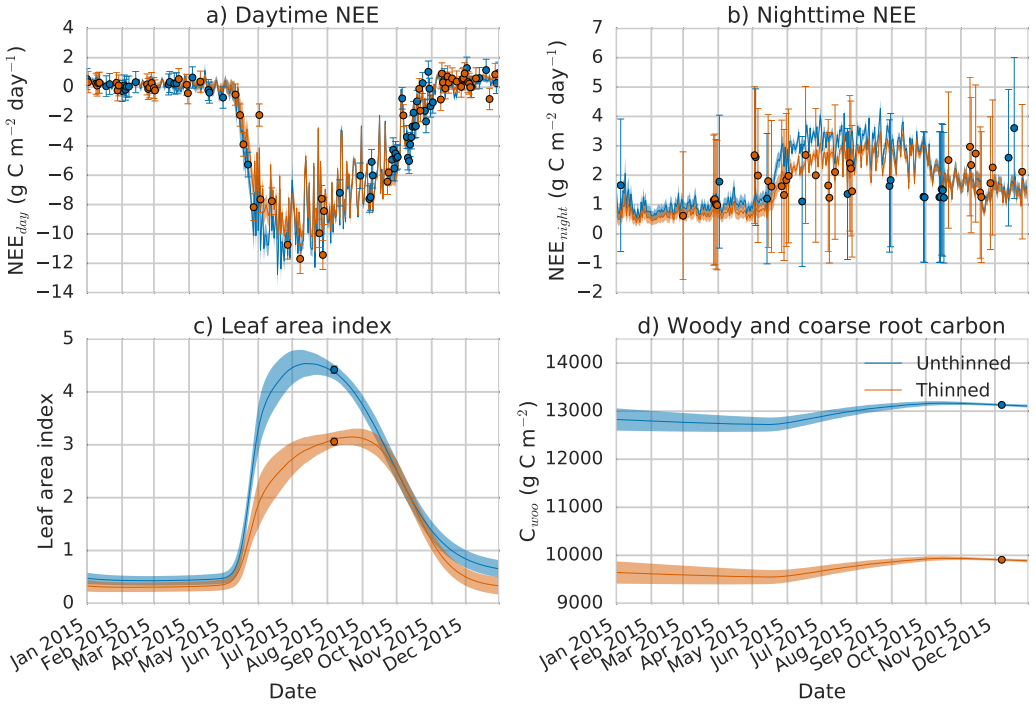

Figure 4. Experiment C: 2015 unthinned and thinned forest observations and model trajectories after assimilation. Colour, lines and dots have the same meaning as described in Figure 3. Figure c) and d) now also include observations of LAI and C_{woo} (dots).

caused an increase in ecosystem respiration and that this had been compensated for by an increase in GPP. This is the opposite conclusion to the one we find in experiment C when we include observations relating to the structure of the forest.

In Figure 6 we show the partitioning of cumulative ecosystem respiration for the year 2015 between total autotrophic respiration and heterotrophic respiration from litter and soil for both the unthinned and thinned forest in experiment C. Here we can see the strong dependance of autotrophic respiration on GPP with the growth rate being much greater between June 2015 - September 2015 (when GPP will be of greater magnitude). For heterotrophic respiration the growth rate is more constant throughout the whole year. Total ecosystem respiration is reduced by 331 g C m^{-2} for the thinned forest when compared to the unthinned forest, with reductions in both heterotrophic and autotrophic respiration of 169 g C m^{-2} and 162 g C m^{-2} respectively.

Figure 7 shows the change in parameter and initial state values for the thinned and unthinned forest after assimilating all observations in experiment C. It is important to note

374 **Table 4.** Root-mean-square error of model fit to observations for the prior model and all experiments after
375 data assimilation.

Unthinned forest				
Exp.	NEE_{day}	NEE_{night}	LAI	C_{woo}
Prior	1.25 g C m^{-2} day^{-1}	1.02 g C m^{-2} day^{-1}	0.43	5507 g C m^{-2}
A	0.61 g C m^{-2} day^{-1}	0.83 g C m^{-2} day^{-1}	2.16	6361 g C m^{-2}
B	0.75 g C m^{-2} day^{-1}	0.93 g C m^{-2} day^{-1}	0.04	5987 g C m^{-2}
C	0.75 g C m^{-2} day^{-1}	0.93 g C m^{-2} day^{-1}	0.04	0.16 g C m^{-2}
Thinned forest				
Exp.	NEE_{day}	NEE_{night}	LAI	C_{woo}
Prior	1.05 g C m^{-2} day^{-1}	0.61 g C m^{-2} day^{-1}	1.79	2285 g C m^{-2}
A	0.63 g C m^{-2} day^{-1}	0.54 g C m^{-2} day^{-1}	0.55	2505 g C m^{-2}
B	0.63 g C m^{-2} day^{-1}	0.56 g C m^{-2} day^{-1}	0.04	2241 g C m^{-2}
C	0.63 g C m^{-2} day^{-1}	0.56 g C m^{-2} day^{-1}	0.04	0.07 g C m^{-2}

422 that this is the difference when compared to our prior model estimate, which was found
423 by assimilating only eddy covariance, LAI and leaf mass per area observations from 2012
424 and 2013. We therefore expect changes in parameter and state values for both the thinned
425 and unthinned forest, as we are assimilating new data streams. This is particularly no-
426 ticeable in the carbon pool state variables in Figure 7. Constraints on the carbon pool
427 state variables are provided by the assimilated observations of woody biomass and coarse
428 roots (C_{woo}), LAI and leaf mass per area (c_{lma}). LAI and c_{lma} give us a constraint on
429 foliar carbon (C_{fol}) as LAI = $\frac{C_{fol}}{c_{lma}}$. We can see the values for the model predicted car-
430 bon pools are as we might expect with the thinned forest having less carbon in all pools
431 when compared to the unthinned forest. For litter carbon (C_{lit}) we expect a reduction in
432 input of leaf litter for the thinned forest and, although there might be increased woody
433 debris after thinning, this is much less readily decomposed and so possibly has little im-
434 pact in the year after thinning [*Wilkinson et al.*, 2016]. The difference in predicted soil

401 **Table 5.** Total annual fluxes and standard deviations for 2015 after assimilation (g C m^{-2}).

Unthinned forest			
Flux	Experiment A	Experiment B	Experiment C
NEE	−379 ± 99	−425 ± 113	−426 ± 116
GPP	1648 ± 159	2191 ± 87	2193 ± 83
TER	1267 ± 150	1766 ± 146	1767 ± 146
Thinned forest			
Flux	Experiment A	Experiment B	Experiment C
NEE	−394 ± 81	−421 ± 73	−420 ± 78
GPP	1976 ± 112	1855 ± 75	1856 ± 80
TER	1582 ± 134	1435 ± 100	1436 ± 109

435 carbon content (C_{som}) between the thinned and unthinned forest is consistent with studies
436 analysing soil carbon contents after felling [*Hernesmaa et al.*, 2005]. For the parameters
437 the biggest changes appear to be in the litter carbon turnover rate parameter (θ_{lit}), with
438 the retrieved parameter being significantly reduced for the unthinned forest when com-
439 pared to the thinned. However, we still see reduced total litter respiration in Figure 6 for
440 the thinned forest compared to the unthinned forest. This is due to the significant differ-
441 ence in litter carbon content (C_{lit}) for both sides, with the unthinned forest having a much
442 higher litter carbon content than the thinned forest. The large change in the θ_{lit} parameter
443 between the two sides is therefore compensating for an overestimated difference in litter
444 carbon content between the two sides.

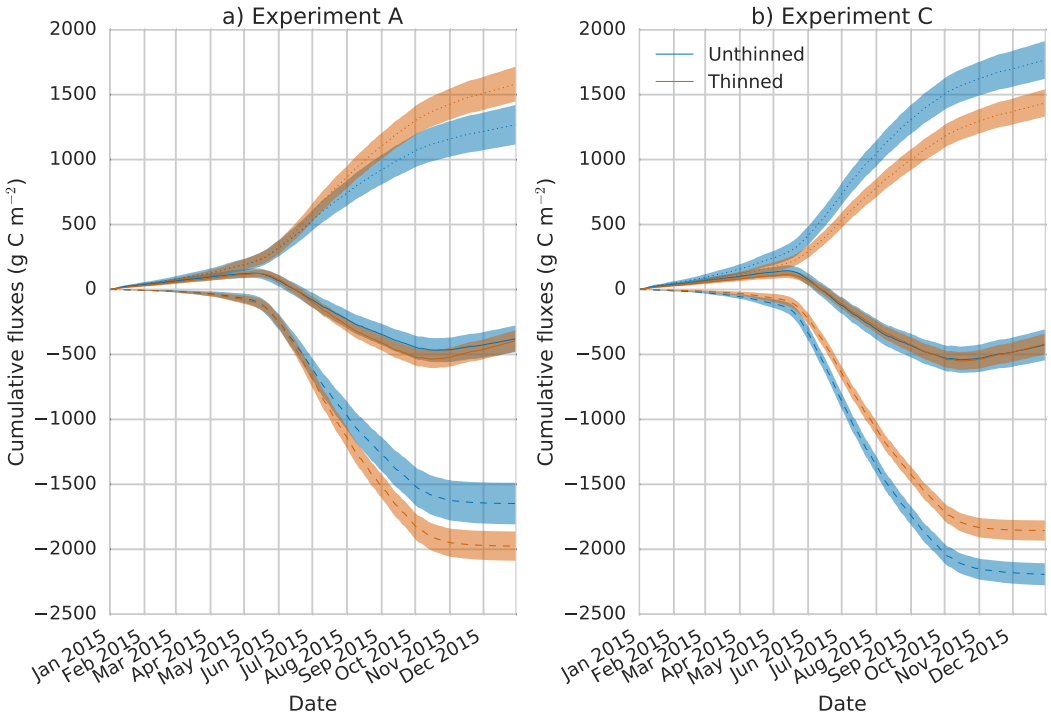

402 **Figure 5.** Experiment A & C: 2015 unthinned and thinned forest model trajectories for cumulative fluxes
403 after assimilation. Solid line: cumulative NEE, dotted line: cumulative ecosystem respiration, dashed line:
404 cumulative GPP. Colour and shading has the same meaning as in Figure 3.

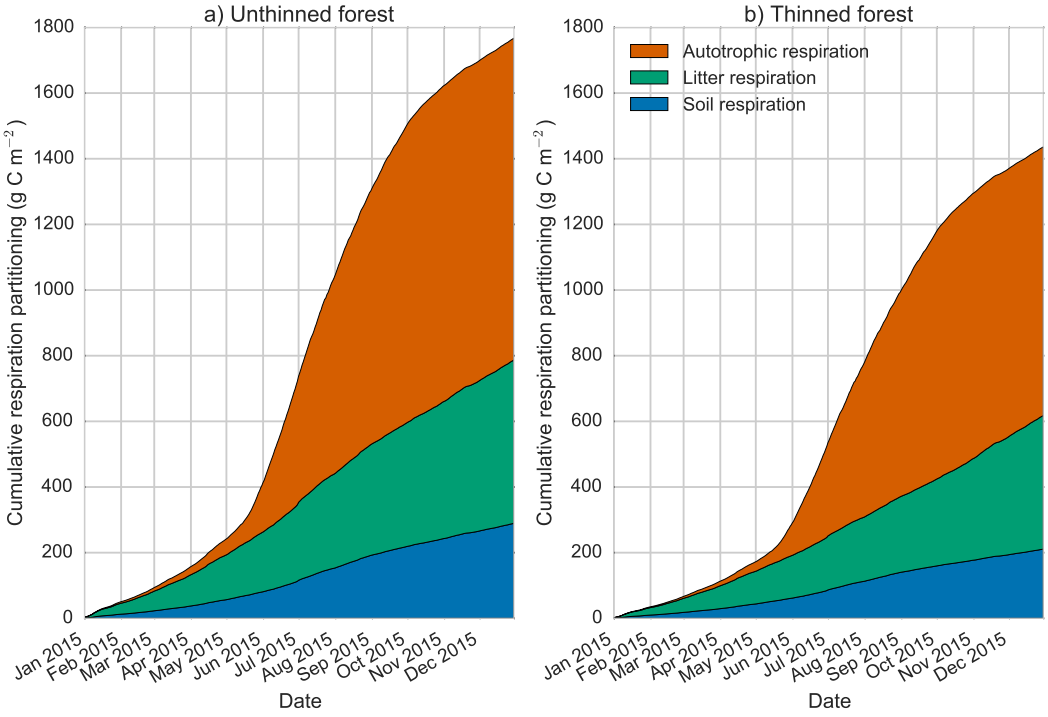

405 **Figure 6.** Experiment C: 2015 unthinned and thinned forest model trajectory for cumulative total ecosys-
406 tem respiration after assimilation and its partitioning between total autotrophic respiration and heterotrophic
407 respiration from litter and soil.

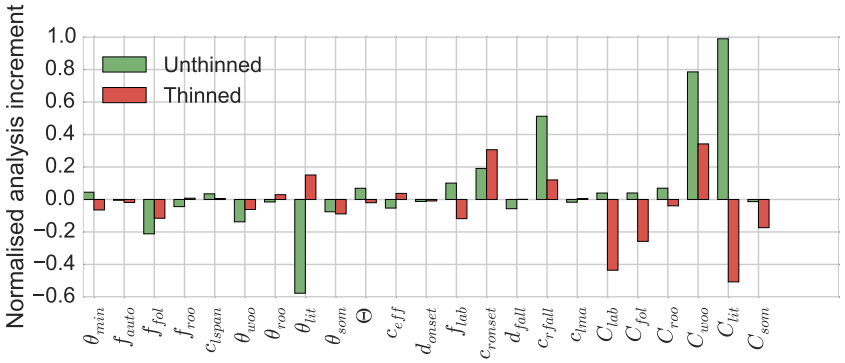

417 **Figure 7.** Experiment C: normalised change in parameter and state variables after data assimilation
418 $(\frac{(\mathbf{x}^a(j)-\mathbf{x}^b(j))}{\mathbf{x}^b(j)})$ for the unthinned and thinned forest. Explanation of parameter and state variable symbols
419 in table A.1.

4 Discussion

In this paper we have used data assimilation to combine observations and prior model predictions of ecosystem carbon balance in order to understand how the state of an ecosystem might be altered after a disturbance event. We conducted three experiments assimilating different combinations of available data streams. For all experiments we find no significant change in net carbon uptake for the studied ecosystem following stand thinning, where approximately 46% of trees were removed. This is consistent with other studies of ecosystem carbon dynamics following thinning. We find different reasons for this unchanged carbon uptake dependent on which data streams are assimilated. When only assimilating NEE observations we find increased ecosystem respiration and increased GPP post-disturbance. These results are unreliable due to bias introduced into the NEE dataset from partitioning between the thinned and unthinned forest. From our most confident estimate, where all available observations are assimilated, the model shows that reductions in GPP, following a decrease in total leaf area post-thinning, are being offset by simultaneous reductions in ecosystem respiration. This is in contrast to current suggestions that reduced canopy photosynthesis is compensated for by increased GPP by ground vegetation post-thinning [*Vesala et al.*, 2005; *Moreaux et al.*, 2011; *Dore et al.*, 2012; *Wilkinson et al.*, 2016].

Our results show a decrease in both autotrophic and heterotrophic respirations following thinning. Autotrophic respiration has both above and below ground components, whereas heterotrophic respiration is mainly from soils and litter. We follow the definition of *Heinemeyer et al.* [2012] and characterise below ground autotrophic respiration as respiration from roots, mycorrhizal fungi and other micro-organisms dependent on the priming of soils with labile carbon compounds from roots. It has been shown recently that deep root systems and their influences may be more widespread than previously thought [*Pierret et al.*, 2016]. Heterotrophic respiration is respiration by microbes not directly dependent on autotrophic substrate; however, the largest fraction of heterotrophic respiration is based on the decomposition of young organic matter (e.g. leaves and fine roots) whose availability also depends on the GPP of an ecosystem [*Janssens et al.*, 2001]. We find similar decreases in both heterotrophic and autotrophic respiration for the thinned forest when compared with the unthinned forest. While it has been shown that heterotrophic respiration can decrease after disturbance events [*Bhupinderpal et al.*, 2003], it is possible we overestimate the reduction in heterotrophic respiration and underestimate the reduction

in autotrophic respiration. This is understandable as we have assimilated no data on this partitioning. Also our model description of autotrophic respiration is simple (described as a constant fraction of GPP) and therefore the heterotrophic respiration component of the model might compensate and in this instance describe the behaviour of mycorrhizal fungi and other microbes commonly categorised in the autotrophic component of respiration.

In a study measuring soil CO_2 fluxes over 4 years at the Straits Inclosure (the study site in this paper) *Heinemeyer et al.* [2012] showed a large 56% contribution of autotrophic respiration (characterised as root and mycorrhizal respiration) to total measured soil respiration. *Heinemeyer et al.* [2012] also suggested that mycorrhizal fungi play a role in priming the turnover of soil organic carbon by other microbes, with evidence from *Talbot et al.* [2008]. *Högberg and Read* [2006] find similar figures for the autotrophic contribution to total soil respiration, with around half or more of all soil respiration being driven by recent photosynthesis. *Heinemeyer et al.* [2012] discuss the possibility of this tight coupling between GPP and ecosystem respiration leading to an upper limit for forest CO_2 uptake due to increased GPP leading to increased respiration, which is also discussed by *Heath et al.* [2005]. Our results support this hypothesis, as ecosystem respiration scales with GPP after approximately 46% of trees are removed from the study site, meaning that we find no significant change in net ecosystem carbon uptake after thinning.

Studies analysing eddy covariance flux records also find no significant change in the net ecosystem exchange of CO_2 after thinning [*Vesala et al.*, 2005; *Moreaux et al.*, 2011; *Dore et al.*, 2012; *Wilkinson et al.*, 2016]. These studies hypothesise that the unchanged NEE is due to increased GPP by ground vegetation (following increased light availability and reduced competition) compensating for increases in heterotrophic respiration and reduced canopy photosynthesis post-thinning. We do not find evidence to support such hypothesis and instead suggest that reduced ecosystem respiration is the most important component for the unchanged NEE of the forest following thinning. However, it is important to note that our measurements of LAI are made at approximately 1 m above the forest floor, which means that our measurements of LAI do not account for ground vegetation. Therefore, any effect of this ground vegetation is not simulated by our model. Despite this, observations made during multiple walks of the three established transects find no evidence of increased ground vegetation in the year after thinning. In fact much of the ground vegetation and subcanopy was removed during thinning and did not appear to have recovered in the following year. At longer time-scales re-growth of the subcanopy

and ground vegetation will play an important role in increased productivity. Our results suggest that this increased productivity would also be met with subsequent increases in ecosystem respiration.

The effect of disturbance is poorly characterised in current land surface and global climate models [*Running*, 2008]; it is important to better understand how parameters and carbon pools might change following disturbance. DALEC2 and many other ecosystem models assume that respiration rates are proportional to carbon pool size. It has been suggested that although this assumption works well in equilibrium conditions it may not allow such models to predict ecosystem carbon dynamics following disturbance [*Schimel and Weintraub*, 2003]. The data assimilation techniques in this paper present a way for these simple models to cope with step changes in ecosystem behaviour, by allowing parameters and carbon pools to be updated following disturbance events.

5 Conclusion

In this work we have presented novel methods for understanding ecosystem responses to disturbance by using data assimilation. Assimilating all available data streams after an event of disturbance with a prior model prediction allows us to assess changes to model parameter and state variables due to this disturbance. We have also created modified observation operators to allow for the assimilation of daytime and nighttime NEE observations with a daily time-step model. This negated the need for model modification and increased the number of observations by a factor of 4.25.

Our modelled estimates show no significant change in net ecosystem carbon uptake after a thinning event in 2014 where approximately 46% of trees were removed from the studied area. Similar results were also found following a thinning activity in 2007 [*Wilkinson et al.*, 2016]. From our optimised model we find that reduced ecosystem respiration is the main reason for this unchanged net ecosystem carbon uptake. Therefore, even for a decrease in GPP following thinning, there is no significant change in NEE. We hypothesise this reduction in ecosystem respiration is due to reduced input of autotrophic substrate following thinning, meaning both autotrophic and heterotrophic respiration are reduced. These results support work suggesting that GPP is the dominant driver for ecosystem respiration [*Janssens et al.*, 2001; *Bhupinderpal et al.*, 2003; *Högberg and Read*, 2006; *Heinemeyer et al.*, 2012; *Moore et al.*, 2013]. This has implications for future predictions of land

surface carbon uptake and whether forests will continue to sequester atmospheric CO_2 at similar rates, or if they will be limited by increased GPP leading to increased respiration.

A: Appendix

A.1 DALEC2 equations

The model equations for the carbon pools at day i are as follows:

$$GPP^i = ACM(C_{fol}^{i-1}, c_{lma}, c_{eff}, \Psi) \tag{A.1}$$

$$C_{lab}^i = C_{lab}^{i-1} + (1 - f_{auto})(1 - f_{fol}) f_{lab} GPP^i - \Phi_{on} C_{lab}^{i-1}, \tag{A.2}$$

$$C_{fol}^i = C_{fol}^{i-1} + \Phi_{on} C_{lab}^{i-1} + (1 - f_{auto}) f_{fol} GPP^i - \Phi_{off} C_{fol}^{i-1}, \tag{A.3}$$

$$C_{roo}^i = C_{roo}^{i-1} + (1 - f_{auto})(1 - f_{fol})(1 - f_{lab}) f_{roo} GPP^i - \theta_{roo} C_{roo}^{i-1}, \tag{A.4}$$

$$C_{woo}^i = C_{woo}^{i-1} + (1 - f_{auto})(1 - f_{fol})(1 - f_{lab})(1 - f_{roo}) GPP^i - \theta_{woo} C_{woo}^{i-1}, \tag{A.5}$$

$$C_{lit}^i = C_{lit}^{i-1} + \theta_{roo} C_{roo}^{i-1} + \Phi_{off} C_{fol}^{i-1} - (\theta_{lit} + \theta_{min}) e^{\Theta T^{i-1}} C_{lit}^{i-1}, \tag{A.6}$$

$$C_{som}^i = C_{som}^{i-1} + \theta_{woo} C_{woo}^{i-1} + \theta_{min} e^{\Theta T^{i-1}} C_{lit}^{i-1} - \theta_{som} e^{\Theta T^{i-1}} C_{som}^{i-1}, \tag{A.7}$$

where T^{i-1} is the daily mean temperature, Ψ represents the meteorological driving data used in the GPP function and Φ_{on}/Φ_{off} are functions controlling leaf-on and leaf-off. Descriptions for each model parameter used in equations (A.1) to (A.7) are included in table A.1. DALEC2 can be parameterised for both deciduous and evergreen sites with Φ_{on} and Φ_{off} being able to reproduce the phenology of either type of site. The full details of this version of DALEC can be found in *Bloom and Williams* [2015].

Acknowledgments

This work was funded by the UK Natural Environment Research Council (NE/K00705X/1) with a CASE award from the UK Forestry Commission. This work was also partly funded by the National Centre for Earth Observation. We are grateful to Ian Craig for providing Forest Research mensuration estimates.

Code and data available at: https://github.com/dalec-reading/4dvar_dalec_alice_holt

553 **Table A.1.** Parameter values and standard deviations for prior vector used in experiments.

Parameter	Description	Prior estimate ($\mathbf{x}^b$)	Standard deviation	Range
θ_{min}	Litter mineralisation rate (day^{-1})	5.471×10^{-4}	6.828×10^{-7}	10^{-5} – 10^{-2}
f_{auto}	Autotrophic respiration fraction	4.492×10^{-1}	1.814×10^{-4}	0.3 – 0.7
f_{fol}	Fraction of GPP allocated to foliage	4.091×10^{-2}	1.211×10^{-4}	0.01 – 0.5
f_{roo}	Fraction of GPP allocated to fine roots	3.700×10^{-1}	3.389×10^{-3}	0.01 – 0.5
c_{lspan}	Determines annual leaf loss fraction	1.089×10^{0}	2.777×10^{-3}	1.0001 – 10
θ_{woo}	Woody carbon turnover rate (day^{-1})	1.012×10^{-4}	3.040×10^{-9}	2.5×10^{-5}–10^{-3}
θ_{roo}	Fine root carbon turnover rate (day^{-1})	5.411×10^{-3}	1.353×10^{-6}	10^{-4} – 10^{-2}
θ_{lit}	Litter carbon turnover rate (day^{-1})	4.387×10^{-3}	1.825×10^{-6}	10^{-4} – 10^{-2}
θ_{som}	Soil and organic carbon turnover rate (day^{-1})	1.311×10^{-4}	2.705×10^{-9}	10^{-7} – 10^{-3}
Θ	Temperature dependance exponent factor	9.354×10^{-2}	6.810×10^{-5}	0.018 – 0.08
c_{eff}	Canopy efficiency parameter	5.618×10^{1}	6.676×10^{0}	10 – 100
d_{onset}	Leaf onset day (day)	1.584×10^{2}	1.370×10^{1}	1 – 365
f_{lab}	Fraction of GPP allocated to labile carbon pool	7.927×10^{-2}	1.491×10^{-4}	0.01 – 0.5
c_{ronset}	Labile carbon release period (days)	1.891×10^{1}	6.011×10^{1}	10 – 100
d_{fall}	Leaf fall day (day)	3.049×10^{2}	1.046×10^{2}	1 – 365
c_{rfall}	Leaf-fall period (days)	5.447×10^{1}	1.502×10^{2}	10 – 100
c_{lma}	Leaf mass per area (g C m^{-2})	2.929×10^{1}	7.099×10^{2}	10 – 400
C_{lab}	Labile carbon pool (g C m^{-2})	7.309×10^{1}	1.672×10^{3}	10 – 1000
C_{fol}	Foliar carbon pool (g C m^{-2})	1.313×10^{1}	6.707×10^{2}	10 – 1000
C_{roo}	Fine root carbon pool (g C m^{-2})	2.103×10^{2}	2.024×10^{4}	10 – 1000
C_{woo}	Above and below ground woody carbon pool (gCm^{-2})	7.182×10^{3}	2.019×10^{7}	100 – 10^{5}
C_{lit}	Litter carbon pool (g C m^{-2})	1.697×10^{2}	4.958×10^{4}	10 – 1000
C_{som}	Soil and organic carbon pool (g C m^{-2})	1.950×10^{3}	8.344×10^{5}	100 – 2×10^{5}

References

Bhupinderpal, S., A. Nordgren, M. Ottosson Löfvenius, M. N. Högberg, P. E. Mellander, and P. Högberg (2003), Tree root and soil heterotrophic respiration as revealed by girdling of boreal scots pine forest: extending observations beyond the first year, *Plant, Cell & Environment*, *26*(8), 1287–1296, doi:10.1046/j.1365-3040.2003.01053.x.

Bloom, A. A., and M. Williams (2015), Constraining ecosystem carbon dynamics in a data-limited world: integrating ecological "common sense" in a model?Äìdata fusion framework, *Biogeosciences*, *12*(5), 1299–1315, doi:10.5194/bg-12-1299-2015.

Braswell, B. H., W. J. Sacks, E. Linder, and D. S. Schimel (2005), Estimating diurnal to annual ecosystem parameters by synthesis of a carbon flux model with eddy covariance net ecosystem exchange observations, *Global Change Biology*, *11*(2), 335–355.

Bréda, N. J. (2003), Ground-based measurements of leaf area index: a review of methods, instruments and current controversies, *Journal of experimental botany*, *54*(392), 2403–2417.

Ciais, P., C. Sabine, G. Bala, L. Bopp, V. Brovkin, J. Canadell, A. Chhabra, R. DeFries, J. Galloway, M. Heimann, et al. (2014), Carbon and other biogeochemical cycles, in *Climate change 2013: the physical science basis. Contribution of Working Group I to the Fifth Assessment Report of the Intergovernmental Panel on Climate Change*, pp. 465–570, Cambridge University Press.

Dahdouh-Guebas, F., and N. Koedam (2006), Empirical estimate of the reliability of the use of the point-centred quarter method (pcqm): Solutions to ambiguous field situations and description of the pcqm+ protocol, *Forest Ecology and management*, *228*(1), 1–18.

Dijkstra, F. A., and W. Cheng (2007), Interactions between soil and tree roots accelerate long-term soil carbon decomposition, *Ecology Letters*, *10*(11), 1046–1053, doi:10.1111/j.1461-0248.2007.01095.x.

Dore, S., M. Montes-Helu, S. C. Hart, B. A. Hungate, G. W. Koch, J. B. Moon, A. J. Finkral, and T. E. Kolb (2012), Recovery of ponderosa pine ecosystem carbon and water fluxes from thinning and stand-replacing fire, *Global change biology*, *18*(10), 3171–3185.

Fassnacht, K. S., S. T. Gower, J. M. Norman, and R. E. McMurtric (1994), A comparison of optical and direct methods for estimating foliage surface area index in forests, *Agricultural and Forest Meteorology*, *71*(1), 183–207.

Fox, A., M. Williams, A. D. Richardson, D. Cameron, J. H. Gove, T. Quaife, D. Ricciuto, M. Reichstein, E. Tomelleri, C. M. Trudinger, et al. (2009), The reflex project: comparing different algorithms and implementations for the inversion of a terrestrial ecosystem model against eddy covariance data, *Agricultural and Forest Meteorology*, *149*(10), 1597–1615.

Heath, J., E. Ayres, M. Possell, R. D. Bardgett, H. I. Black, H. Grant, P. Ineson, and G. Kerstiens (2005), Rising atmospheric co2 reduces sequestration of root-derived soil carbon, *Science*, *309*(5741), 1711–1713.

Heinemeyer, A., M. Wilkinson, R. Vargas, J.-A. Subke, E. Casella, J. I. Morison, and P. Ineson (2012), Exploring the "overflow tap" theory: linking forest soil co2 fluxes and individual mycorrhizosphere components to photosynthesis, *Biogeosciences*, *9*(1), 79–95.

Hernesmaa, A., K. Bj??rkl??f, O. Kiikkil?ğ, H. Fritze, K. Haahtela, and M. Romantschuk (2005), Structure and function of microbial communities in the rhizosphere of scots pine after tree-felling, *Soil Biology and Biochemistry*, *37*(4), 777 – 785, doi: http://dx.doi.org/10.1016/j.soilbio.2004.10.010.

Hilker, T., M. A. Wulder, N. C. Coops, J. Linke, G. McDermid, J. G. Masek, F. Gao, and J. C. White (2009), A new data fusion model for high spatial-and temporal-resolution mapping of forest disturbance based on landsat and modis, *Remote Sensing of Environment*, *113*(8), 1613–1627.

Högberg, P., and D. J. Read (2006), Towards a more plant physiological perspective on soil ecology, *Trends in Ecology & Evolution*, *21*(10), 548–554.

Högberg, P., A. Nordgren, N. Buchmann, A. F. Taylor, A. Ekblad, M. N. Högberg, G. Nyberg, M. Ottosson-Löfvenius, and D. J. Read (2001), Large-scale forest girdling shows that current photosynthesis drives soil respiration, *Nature*, *411*(6839), 789–792.

Janssens, I. A., H. Lankreijer, G. Matteucci, A. S. Kowalski, N. Buchmann, D. Epron, K. Pilegaard, W. Kutsch, B. Longdoz, T. Grünwald, L. Montagnani, S. Dore, C. Rebmann, E. J. Moors, A. Grelle, Ü. Rannik, K. Morgenstern, S. Oltchev, R. Clement, J. Guðmundsson, S. Minerbi, P. Berbigier, A. Ibrom, J. Moncrieff, M. Aubinet, C. Bernhofer, N. O. Jensen, T. Vesala, A. Granier, E. D. Schulze, A. Lindroth, A. J. Dolman, P. G. Jarvis, R. Ceulemans, and R. Valentini (2001), Productivity overshadows temperature in determining soil and ecosystem respiration across european forests, *Global Change Biology*, *7*(3), 269–278, doi:10.1046/j.1365-2486.2001.00412.x.

Jonckheere, I., S. Fleck, K. Nackaerts, B. Muys, P. Coppin, M. Weiss, and F. Baret (2004), Review of methods for in situ leaf area index determination Part I. Theories, sensors and hemispherical photography, *Agricultural and Forest Meteorology*, *121*(1-2), 19–35, doi:10.1016/j.agrformet.2003.08.027.

Kantzas, E., S. Quegan, and M. Lomas (2015), Improving the representation of fire disturbance in dynamic vegetation models by assimilating satellite data: a case study over the arctic, *Geoscientific Model Development*, *8*(8), 2597–2609.

Kerr, G., and J. Haufe (2011), Thinning practice: A silvicultural guide, *Forestry Commission*, p. 54.

Kimmins, J. (1973), Some statistical aspects of sampling throughfall precipitation in nutrient cycling studies in british columbian coastal forests, *Ecology*, pp. 1008–1019.

Kurz, W. A., C. Dymond, G. Stinson, G. Rampley, E. Neilson, A. Carroll, T. Ebata, and L. Safranyik (2008), Mountain pine beetle and forest carbon feedback to climate change, *Nature*, *452*(7190), 987–990.

Liu, S., B. Bond-Lamberty, J. A. Hicke, R. Vargas, S. Zhao, J. Chen, S. L. Edburg, Y. Hu, J. Liu, A. D. McGuire, J. Xiao, R. Keane, W. Yuan, J. Tang, Y. Luo, C. Potter, and J. Oeding (2011), Simulating the impacts of disturbances on forest carbon cycling in north america: Processes, data, models, and challenges, *Journal of Geophysical Research: Biogeosciences*, *116*(G4), n/a–n/a, doi:10.1029/2010JG001585, g00K08.

McKay, H., J. Hudson, and R. Hudson (2003), Woodfuel resource in britain, *Forestry Commission Report*.

Moore, D. J. P., N. A. Trahan, P. Wilkes, T. Quaife, B. B. Stephens, K. Elder, A. R. Desai, J. Negron, and R. K. Monson (2013), Persistent reduced ecosystem respiration after insect disturbance in high elevation forests, *Ecology Letters*, *16*(6), 731–737, doi:10.1111/ele.12097.

Moreaux, V., É. Lamaud, A. Bosc, J.-M. Bonnefond, B. E. Medlyn, and D. Loustau (2011), Paired comparison of water, energy and carbon exchanges over two young maritime pine stands (pinus pinaster ait.): effects of thinning and weeding in the early stage of tree growth, *Tree physiology*, p. tpr048.

Morecroft, M. D., V. J. Stokes, and J. I. L. Morison (2003), Seasonal changes in the photosynthetic capacity of canopy oak (quercus robur) leaves: the impact of slow development on annual carbon uptake, *International Journal of Biometeorology*, *47*(4), 221–226, doi:10.1007/s00484-003-0173-3.

Navon, I. (1998), Practical and theoretical aspects of adjoint parameter estimation and identifiability in meteorology and oceanography, *Dynamics of Atmospheres and Oceans*, *27*(1), 55–79.

Niu, S., Y. Luo, M. C. Dietze, T. F. Keenan, Z. Shi, J. Li, and F. S. C. Iii (2014), The role of data assimilation in predictive ecology, *Ecosphere*, *5*(5), art65, doi:10.1890/ES13-00273.1.

Papale, D., M. Reichstein, M. Aubinet, E. Canfora, C. Bernhofer, W. Kutsch, B. Longdoz, S. Rambal, R. Valentini, T. Vesala, et al. (2006), Towards a standardized processing of net ecosystem exchange measured with eddy covariance technique: algorithms and uncertainty estimation, *Biogeosciences*, *3*(4), 571–583.

Pierret, A., J.-L. Maeght, C. ClÈment, J.-P. Montoroi, C. Hartmann, and S. Gonkhamdee (2016), Understanding deep roots and their functions in ecosystems: an advocacy for more unconventional research, *Annals of Botany*, *118*(4), 621–635, doi:10.1093/aob/mcw130.

Pinnington, E. M., E. Casella, S. L. Dance, A. S. Lawless, J. I. Morison, N. K. Nichols, M. Wilkinson, and T. L. Quaife (2016), Investigating the role of prior and observation error correlations in improving a model forecast of forest carbon balance using four-dimensional variational data assimilation, *Agricultural and Forest Meteorology*, *228–229*, 299 – 314, doi:http://dx.doi.org/10.1016/j.agrformet.2016.07.006.

Quaife, T., P. Lewis, M. De Kauwe, M. Williams, B. E. Law, M. Disney, and P. Bowyer (2008), Assimilating canopy reflectance data into an ecosystem model with an Ensemble Kalman Filter, *Remote Sensing of Environment*, *112*(4), 1347–1364, doi:10.1016/j.rse.2007.05.020.

Raupach, M., P. Rayner, D. Barrett, R. DeFries, M. Heimann, D. Ojima, S. Quegan, and C. Schmullius (2005), Model–data synthesis in terrestrial carbon observation: methods, data requirements and data uncertainty specifications, *Global Change Biology*, *11*(3), 378–397.

Reich, P. B., M. B. Walters, and D. S. Ellsworth (1991), Leaf age and season influence the relationships between leaf nitrogen, leaf mass per area and photosynthesis in maple and oak trees, *Plant, Cell & Environment*, *14*(3), 251–259, doi:10.1111/j.1365-3040.1991.tb01499.x.

Rich, P. M., J. Wood, D. Vieglais, K. Burek, and N. Webb (1999), Hemiview user manual, version 2.1, *Delta-T Devices Ltd., Cambridge, UK*, *79*.

691 Richardson, A. D., M. D. Mahecha, E. Falge, J. Kattge, A. M. Moffat, D. Papale, M. Re-
692 ichstein, V. J. Stauch, B. H. Braswell, G. Churkina, B. Kruijt, and D. Y. Hollinger
693 (2008), Statistical properties of random {CO2} flux measurement uncertainty inferred
694 from model residuals, *Agricultural and Forest Meteorology*, *148*(1), 38 – 50, doi:
695 http://dx.doi.org/10.1016/j.agrformet.2007.09.001.

696 Richardson, A. D., M. Williams, D. Y. Hollinger, D. J. Moore, D. B. Dail, E. A. David-
697 son, N. A. Scott, R. S. Evans, H. Hughes, J. T. Lee, et al. (2010), Estimating param-
698 eters of a forest ecosystem c model with measurements of stocks and fluxes as joint
699 constraints, *Oecologia*, *164*(1), 25–40.

700 Running, S. W. (2008), Ecosystem disturbance, carbon, and climate, *Science*, *321*(5889),
701 652–653.

702 Saunders, M., B. Tobin, K. Black, M. Gioria, M. Nieuwenhuis, and B. Osborne (2012),
703 Thinning effects on the net ecosystem carbon exchange of a sitka spruce forest
704 are temperature-dependent, *Agricultural and Forest Meteorology*, *157*, 1 – 10, doi:
705 http://dx.doi.org/10.1016/j.agrformet.2012.01.008.

706 Schimel, J. P., and M. N. Weintraub (2003), The implications of exoenzyme activity on
707 microbial carbon and nitrogen limitation in soil: a theoretical model, *Soil Biology and*
708 *Biochemistry*, *35*(4), 549–563.

709 Seidl, R., P. M. Fernandes, T. F. Fonseca, F. Gillet, A. M. Jönsson, K. Merganičová,
710 S. Netherer, A. Arpaci, J.-D. Bontemps, H. Bugmann, et al. (2011), Modelling natural
711 disturbances in forest ecosystems: a review, *Ecological Modelling*, *222*(4), 903–924.

712 Talbot, J., S. Allison, and K. Treseder (2008), Decomposers in disguise: mycorrhizal fungi
713 as regulators of soil c dynamics in ecosystems under global change, *Functional ecology*,
714 *22*(6), 955–963.

715 Thornton, P., B. Law, H. L. Gholz, K. L. Clark, E. Falge, D. Ellsworth, A. Goldstein,
716 R. Monson, D. Hollinger, M. Falk, et al. (2002), Modeling and measuring the effects
717 of disturbance history and climate on carbon and water budgets in evergreen needleleaf
718 forests, *Agricultural and forest meteorology*, *113*(1), 185–222.

719 Tremolet, Y. (2006), Accounting for an imperfect model in 4D-Var, *Quarterly Journal of*
720 *the Royal Meteorological Society*, *132*(621), 2483–2504, doi:10.1256/qj.05.224.

721 Vesala, T., T. Suni, Ü. Rannik, P. Keronen, T. Markkanen, S. Sevanto, T. Grönholm,
722 S. Smolander, M. Kulmala, H. Ilvesniemi, et al. (2005), Effect of thinning on surface
723 fluxes in a boreal forest, *Global Biogeochemical Cycles*, *19*(2).

Wilkinson, M., E. Eaton, M. Broadmeadow, and J. Morison (2012), Inter-annual variation of carbon uptake by a plantation oak woodland in south-eastern england, *Biogeosciences*, *9*(12), 5373–5389.

Wilkinson, M., P. Crow, E. Eaton, and J. Morison (2015), Effects of management thinning on co_2 exchange by a plantation oak woodland in south-eastern england., *Biogeosciences Discussions*, *12*(19).

Wilkinson, M., P. Crow, E. L. Eaton, and J. I. L. Morison (2016), Effects of management thinning on co2 exchange by a plantation oak woodland in south-eastern england, *Biogeosciences*, *13*(8), 2367–2378, doi:10.5194/bg-13-2367-2016.

Williams, M., E. B. Rastetter, D. N. Fernandes, M. L. Goulden, G. R. Shaver, and L. C. Johnson (1997), Predicting gross primary productivity in terrestrial ecosystems, *Ecological Applications*, *7*(3), 882–894.

Williams, M., P. A. Schwarz, B. E. Law, J. Irvine, and M. R. Kurpius (2005), An improved analysis of forest carbon dynamics using data assimilation, *Global Change Biology*, *11*(1), 89–105.

Zobitz, J., A. Desai, D. Moore, and M. Chadwick (2011), A primer for data assimilation with ecological models using markov chain monte carlo (mcmc), *Oecologia*, *167*(3), 599–611.

Zobitz, J. M., D. J. P. Moore, T. Quaife, B. H. Braswell, A. Bergeson, J. a. Anthony, and R. K. Monson (2014), Joint data assimilation of satellite reflectance and net ecosystem exchange data constrains ecosystem carbon fluxes at a high-elevation subalpine forest, *Agricultural and Forest Meteorology*, *195-196*, 73–88, doi:10.1016/j.agrformet.2014.04.011.